J Solid State Electrochem (2011) 15:1209–1216
DOI 10.1007/s10008-010-1193-7

ORIGINAL PAPER

Long-term durability study of perfluoropolymer membranes in low humidification conditions

Alfonso Pozio · Alessia Cemmi · Francesco Mura · Amedeo Masci · Emanuele Serra · Rodrigo Ferreira Silva

Received: 23 July 2010 / Revised: 2 September 2010 / Accepted: 6 September 2010 / Published online: 17 September 2010

Abstract This paper reports a study on the understanding of the performance decrease mechanisms of polymer electrolyte fuel cells under critical operating conditions. In order to investigate the durability of perfluorosulfonate membranes at low humidification conditions, long-term fuel cell tests have been carried out. Results evidenced a strong effect of low relative humidity on the commercial polymer membrane lifetime. Prolonged dehydration of the membranes led to a decrease of the three-dimensional reaction zone due to the ionomer degradation in the catalytic layer and a continuous loss of material in the membrane evidenced by a thickness decrease. The last effect provoked a collapse of the electrode structure.

Keywords Polymer membrane · PEFC · Degradation · Humidification · Fluoride release

Introduction

Polymer electrolyte fuel cells (PEFCs) based on proton exchange membranes are considered as the leading candidate to replace the traditional power sources like the internal combustion engines and find application in the cogeneration power for both stationary and portable systems. In the cell, fuel is oxidized at the anode, oxygen is reduced to water at the cathode, and electrical energy is delivered with a very high yield in a production process having near-zero emissions. At present, one of the most common perfluorosulfonic acid-based membranes employed in fuel cells is DuPont®'s Nafion®. This membrane has many desirable properties, including good chemical stability, high mechanical strength and high ionic conductivity under high humidity conditions. However, the proton conductivity of perfluorosulfonate membrane is strongly dependent on water content, and it decreases considerably at low relative humidity (RH), leading to large relative losses and a reduction in the cell voltage and efficiency. Long-term experiments can give a good indication of the severity of degradation mechanisms and their relative contribution to performance loss under various conditions [1].

According to Huang et al. [2], when proton exchange membranes are exposed to dry conditions over a long period of time, they can become brittle and develop crazes or cracks. The authors have also stated the necessity of understanding the membrane kinetics and the membrane electrode assembly (MEA) embrittlement process as a function of the local conditions, particularly temperature and relative humidity. Because membrane degradation is probably one of the main factors that reduce the fuel cell lifetime [3], it is important to study it in extreme RH conditions. Besides, operating a fuel cell at low relative humidity can result in several advantages [4]: (1) enablement of operation at elevated T which allows a more efficient heat removal; (2) no gas humidification subsystem is needed; (3) removal of water in vapour form reduces the amount of heat to be removed from the cell by the latent heat of vaporization; and (4) less condensed water, present in the fluid flow channels for the gases in the bipolar plates and gas diffusion electrodes, enhances the fuel cell performance. Therefore, there is a growing interest to develop and commercialize PEFCs that work under these conditions. Very few works were devoted to the long-term

A. Pozio (✉) · A. Cemmi · F. Mura · A. Masci · E. Serra · R. F. Silva
ENEA, C.R. Casaccia,
Via Anguillarese 301, S. Maria di Galeria,
00123 Rome, Italy
e-mail: alfonso.pozio@enea.it

study of in situ membrane performance at low RH [4–7] in constant current mode. In addition, such works have been carried out using different materials (membrane, catalyst, etc.) and operative conditions (current, cell temperature, etc.), so it becomes complicated to understand whether the differences are due only to the effect of RH on the membrane or to the degradation of other components as well.

Buchi and Srinivasan [4] have performed long-term tests on a 50-cm^2 single cell using Nafion® 115 at 50 °C [4]. The level of performance obtained is 20–40% lower than the conventional operation mode with both gases humidified to supersaturation. The authors [4] observed a performance decrease when a voltage of 0.61 V was applied over a period of 1,800 h, and surprisingly, they attributed the observed current decay to factors other than drying out of the cell (for example, impurities in the gases fed to the cell). Yu et al. [5] have conducted a 2,700-h long-term test at 0.3 $A cm^{-2}$ and 75 °C on a 50-cm^2 single cell using Nafion® 112 under partially saturated humidification (RH 80%) and found a decrease of only −2.5 $\mu V h^{-1}$ in the first 1,900 h. Similarly, we have obtained a decrease of only −2.3 $\mu V h^{-1}$ for a 2,000-h long-term test at 0.142 $A cm^{-2}$ and 70 °C performed on a 50-cm^2 single cell with Nafion® 112 (cathode at RH 80% and anode at supersaturated humidification).

In addition, Nakayama et al. [6] have conducted a 950-h long-term test at 0.3 $A cm^{-2}$ and 80 °C on a 45-cm^2 single cell with an unspecified Nafion® membrane at low relative humidity (26%) and measured a decrease of only −28 $\mu V h^{-1}$. On the other hand, Wahdame et al. [7] have performed a 650-h ageing test at higher current (0.5 $A cm^{-2}$) on a three-cell stack at 55 °C using a 100-cm^2 Gore® 5510 membrane under very low humidity (RH 20%) and found a decrease of −217 $\mu V h^{-1}$. Short-side-chain (–$OCF_2CF_2SO_3H$) ionic perfluoropolymers (Solvay Solexis) have also been proposed [8–10] as an alternative to Nafion® long-side-chain (–OCF_2CFCF_3–$OCF_2CF_2SO_3H$) in order to keep operation at higher temperatures, but there are no literature results for long-term tests at low RH.

The RH influence on the short-side-chain (SSC) polymer was only previously supposed by Merlo et al. [10] who observed, through hydrogen crossover measurements, that an increase of the degradation rate was strongly influenced by the low humidification level of the reactants.

As can be seen, literature results for commercial membranes are poor and extremely discordant. In the present work, we aimed at investigating the durability of perfluorosulfonate membranes at low humidification conditions. Assemblies containing two types of commercial membrane were tested in a fuel cell work station to verify the main aspects related to degradation in low humidification conditions and to evaluate strategies for their mitigation [11, 12]. Long-term fuel cell tests were performed on Nafion® 112 and Solvay SSC polymer in order to measure the real degradation rate and to give a possible explanation for the observed phenomena.

Experimental

Materials

Commercially available 30 wt.% Pt/C catalyst powders on carbon black (Vulcan XC72) were purchased from E-Tek Inc. Three-layer (substrate/diffusive layer/catalyst layer) gas diffusion anode and cathode were prepared using a spray technique described in detail in a previous work [13]. The substrate was carbon paper (Toray TGPH090). The weight composition of the diffusion layer was 50 wt.% of carbon and 50 wt.% of PTFE, with carbon loading of about 2.5 mg cm^{-2}. The catalyst layer was prepared by mixing appropriate amounts of carbon-supported catalyst (30 wt.%) and 5 wt.% Nafion® ionomer solution from Aldrich. The platinum loading in all anodes and cathodes was kept constant at 0.54 $mg cm^{-2}$, together with a Nafion® amount of 0.9 $mg cm^{-2}$. The MEAs were prepared using different polymeric electrolyte commercial membranes: Nafion® 112 with an equivalent weight (EW) of 1,020 [11] and Solvay SSC with EW of 870, both with a hydrated nominal thickness of 50 μm. The membranes were used after purification treatment in 5% (*w*/*v*) H_2O_2 solution at 80 °C for 1 h, followed by a second treatment in 1 M H_2SO_4. The MEAs were formed by hot pressing the electrodes (2 cm^2) onto the membrane at 130 °C for 1–5 min and 50–100 kg cm^{-2}.

Physicochemical characterisation

Long-term electrochemical tests have been carried out in a 2-cm^2 active area single cell FC2/40 Fuelcon quickConnect (Germany). The cell was inserted in a Globe Tech Inc. mod. 850C station equipped with an integrated frequency resistance analyzer for high-frequency resistance and an electrochemical impedance spectroscopy equipment.

The cells were fed with low humidified H_2/O_2 gases (RH 23%) under a pressure of 2 bar abs and a stoichiometric ratio of 1:2. The MEAs were submitted to galvanostatic polarization by means of a programmable power supply interfaced with a computer for data acquisition. All the measurements were performed in the same operative conditions. The ohmic cell resistance was also measured continuously by the periodic current pulse transient [14]. In this kind of measurement, the cell current is rapidly removed and the cell voltage sampled after a time delay of 20 μs.

Long-term tests were carried out on MEA assemblies at 50 °C and 250 $mA cm^{-2}$ in H_2/O_2 flux at 50 and 100 ml

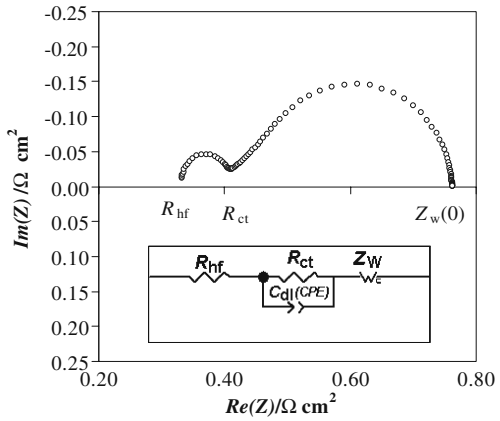

Fig. 1 Nyqvist plot corresponding to the inset equivalent electrical circuit [15] used for impedance PEFC data: high-frequency resistance (R_{hf}), charge transfer resistance (R_{ct}), Warburg impedance (Z_w), double-layer capacitance (C_{dl}) and constant phase element (*CPE*)

min^{-1}, respectively. In order to simulate periodic start-ups and to study the effect of such parameters on membrane ageing, the cell was switched off and left in air at room temperature overnight or sometimes for an entire weekend. Cell voltage vs. time plots were recorded continuously and impedance spectra were periodically acquired in the galvanostatic mode with a DC current of 250 $mA\,cm^{-2}$ and AC 10% DC between 10-kHz and 1-Hz frequency. Periodically, polarization curves were performed at RH 100% for H_2 and 46% for O_2 in order to evaluate changes in the whole cell performance.

Water samples were collected periodically at the exhausts using plastic containers and stored for analysis, and their conductivity was measured by means of a Crison mod. 525 conductivity meter. The fluoride amount released into the product water was determined using a Mettler Toledo F^- ion-selective electrode. The thicknesses of the as-prepared samples as well as those submitted to long-term tests were acquired with a JEOL mod. JSM5510LV scanning electron microscope.

Impedance model

Like other electrochemical cells, a polymer electrolyte fuel cell can be modelled as an equivalent electrical circuit [14] and, as reported by Danzer and Hofer [15], its impedance can be fitted well with a typical model as that represented in the inset of Fig. 1. Such impedance model was used to describe the fuel cell electrochemical behaviour in our frequency range and operating conditions, since it presents a concise mathematical structure. The model is able to fit the measured impedance spectrum, yields a very small error over the whole frequency range, and incorporates a minimum number of parameters.

Here, the R_{hf} element obtained as the intersection of the impedance spectrum with the real axis for $\omega\rightarrow\infty$ approximately corresponds to the ohmic resistance which, in this case, is mainly due to: (1) the proton transport resistance of the membrane (R_{memb}) and (2) the ohmic resistance of current collector plates and electrode graphite (R_{cell}).

In a PEFC, the cathode polarization resistance is much larger than that of the anode; therefore, the circuit model can omit the anode elements. In the used model, the double-layer capacity, C_{dl}, and resistance, R_{ct}, should be referred mainly to the cathode and are a measurement of the charge transfer resistance of the oxygen reduction reaction (ORR) and the interfacial capacitance of the cathode, respectively. The characteristic single loop at high frequency (Fig. 1) is a fairly good indicator of the properties of the cathode, such as the catalyst surface area, catalyst loading and catalyst utilization. In our case, the conventional double-layer capacity is replaced by a constant phase element (CPE) [10, 13]. The CPE is strictly related to the capacitance, being defined by two parameters, Y° and n. If $n = 1$, then the equation is identical to that of a capacitor.

$$C_{dl} = Y^\circ \omega^{n-1} \quad (1)$$

In the case of our model, the CPE was used in place of a capacitor to compensate the non-homogeneity in the system because the capacitance caused by the double-layer charg-

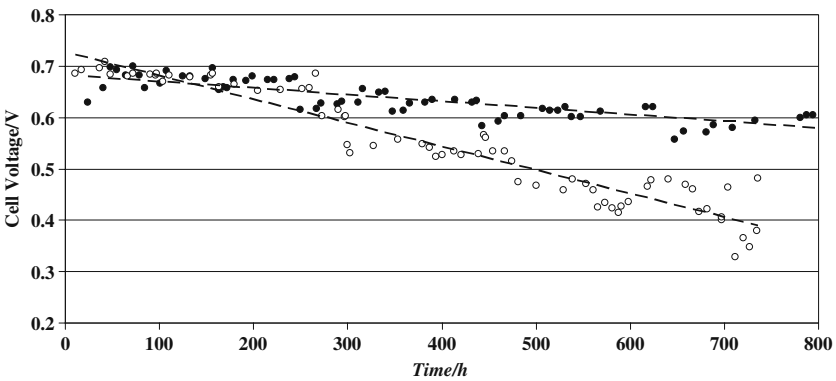

Fig. 2 Cell voltage vs. time plot of MEA with Nafion® 112 (*filled circle*) and SSC polymer (*empty circle*) at 250 $mA\,cm^{-2}$

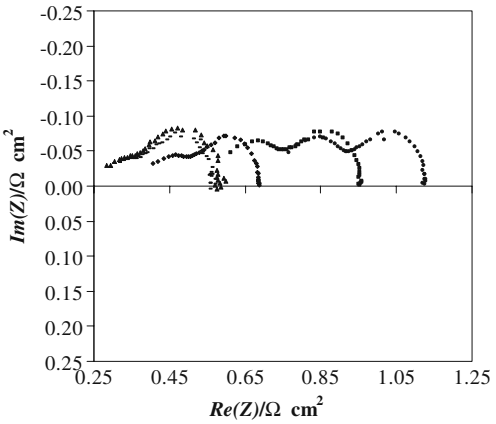

Fig. 3 Nyquist plots of MEA with Nafion® 112 at 50 °C and 250 mA cm^{-2} after 40 h (*triangle*), 48 h (*solid bar*) 179 h (*diamond*) 617 h (*square*), and 1,019 h (*circle*)

ing is distributed along the pore length in the PEFC porous electrode.

Finally, the element Z_W represents the finite-length Warburg impedance. This element was incorporated into the model [15] to account for all the transport effect. Because of the Warburg impedance, this model is able to describe the depressed semicircles. The second low-frequency arc in the Nyquist plot (Fig. 1) is related to this slow mass transport (mainly oxygen) and can be described by the finite-length Warburg impedance (Z_w), as in Eq. 2 [13]:

$$Z_W(\omega) = Z_W(0)\frac{\tanh\lfloor L\sqrt{j\omega D}\rfloor}{L\sqrt{j\omega D}} \quad (2)$$

where ω is the frequency, L the thickness of diffusion layer and D the diffusion coefficient of electroactive species, respectively. The mass transport resistance, $Z_W(0)$ (i.e. $Z_W(\omega)$ when $\omega \to 0$), can be obtained from Eq. 3:

$$Z_W(0) = \frac{RTL}{n^2F^2DC} \quad (3)$$

where R is the gas constant, n is the electron number, F is the Faraday constant, and C is the concentration of the diffusion species. All the values of these equivalent circuit components are a function of the cell operating current or voltage.

Results and discussion

Figure 2 depicts the cell voltage vs. time curves of MEAs prepared with N112 and SSC polymer membranes under particular conditions of low humidity (RH 23%). For N112, the MEA performance at 50 °C and current density of 250 mAcm^{-2} decreases at a rate of −129 μVh^{-1} after 1,024 h with an average voltage of 0.63±0.04 V; however, in the first 600 h, a slightly higher decay (−154 μVh^{-1}) was observed. Further analysis showed that in the first hours, a voltage increase until a maximum of 0.7 V has been reached in about 72 h, and the voltage was kept constant until about 180 h. In the same conditions, the MEA with SSC polymer decreased at a rate of −451 μVh^{-1} after 736 h with an average voltage of 0.55±0.10 V. Also in this case, in the first hours, an increase until a maximum of 0.71 V has been reached in about 40 h, and it was kept constant until about 100 h. In the first 266 h, the decrease was only −104 μVh^{-1}, and subsequently, a sharp decay was observed.

For a better understanding of the phenomena involved, impedance vs. time plots were acquired for the two cells. Figures 3 and 4 show the Nyquist plots for the two membranes in different periods of time.

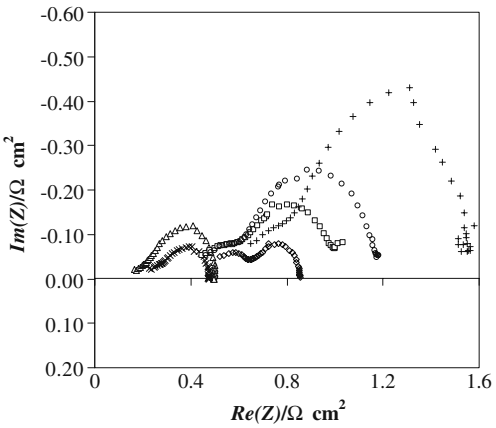

Fig. 4 Nyquist plots of MEA with SSC polymer at 50 °C and 250 mA/cm^2 after 5 h (*triangle*), 17 h (*ex*), 273 h (*diamond*), 474 h (*square*), 641 h (*circle*) and 734 h (*plus sign*)

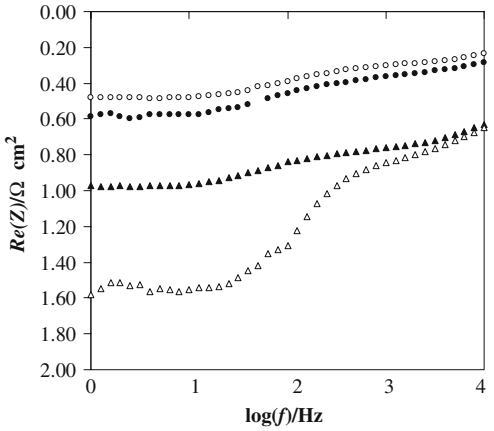

Fig. 5 Bode plot of MEA with N112 (*filled*) and SSC polymer (*empty*) at 50 °C and 250 mA/cm^2 after 40 h (*filled circle* and *empty circle*) and 734 h (*filled triangle* and *empty triangle*)

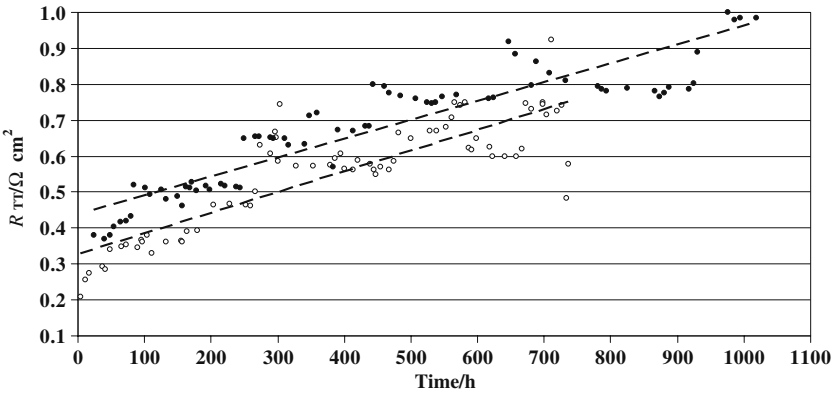

Fig. 6 Current interrupt resistance vs. time plot of MEA with N112 (*filled circle*) and the SSC polymer (*empty circle*) at 250 $mA\,cm^{-2}$

The Nyquist plots were characterized by the presence of two arcs at different frequencies. To explain the impedance behaviour, we have carried out a deeper analysis based on the model relative to the above-described equivalent electric circuit [15].

The contributions of the current collector plates and graphite were estimated by measuring the resistance of the cell fixture with two pieces of Toray carbon paper inserted and clamped with the same pressure of the MEAs; an R_{cell} value of 0.3 Ωcm^2 was obtained due to the ohmic resistance of the current collector plates and graphite electrode.

In the first hours (Figs. 3 and 4), all the impedance components decreased, except R_{hf} which increased mainly in the case of the SSC polymer. This behaviour, known in the initial working stage as "activation process", can be explained considering the water production in the cathode catalytic layer and its effect on the whole conductive polymer phase. Equations 4 and 5 evidence the importance of diffusion of water into the polymeric phase ($H_2O_{polymer}$) and its role in both the electrode reactions.

$$H_2 + 2H_2O_{polymer} \rightarrow 2H_3O^+{}_{polymer} + 2e \quad (4)$$

$$1/2O_2 + 2H_3O^+{}_{polymer} + 2e \rightarrow 3H_2O_{polymer} \quad (5)$$

In the first hours, we have observed a polarization resistance decrease for two of the main contributions (activation R_{ct} and diffusive W) due especially to hydration of the perfluorosulphonate membrane (ionomer and polymer) in direct contact with the catalyst.

A deep analysis of the impedance Bode (Fig. 5) shows that a first dramatic change occurred during the long-term test after the early hours with a continuous increase of R_{hf} in the real part.

The R_{hf} increase is directly related to the growth of the R_{memb} component due to membrane degradation in terms of protonic conductivity reduction. Figure 6 shows the resistance measured by means of a transient technique (R_{TT}) for both samples. As reported by Yuan et al. [14], the impedance and the current interruption method do not generate the same results, and it has been stated [16] that the membrane resistance measured with the current interruption method is closer to the real values.

We have found that both cells showed a linear and irreversible increase: $0.52\pm0.03\ m\Omega cm^{-2}h^{-1}$ for N112 and $0.58\pm0.04\ m\Omega cm^{-2}h^{-1}$ for the SSC polymer. The use of the continuous current interrupt technique demonstrated to be very useful in order to evaluate the fuel cell long-term behaviour. In fact, considering the reported R_{cell} value, the in situ low RH membrane resistance, R_{memb}, and the corresponding conductivity (σ) were easily calculated by Eq. 6, where l represents the membrane thickness as a function of working time. We have found a decrease of conductivity from 71.6 to 6.1 $mS\,cm^{-1}$ for N112 and from 103 to 8 $mS\,cm^{-1}$ for the SSC polymer.

$$\sigma = \frac{(R_{TT} - R_{cell})}{l} \quad (6)$$

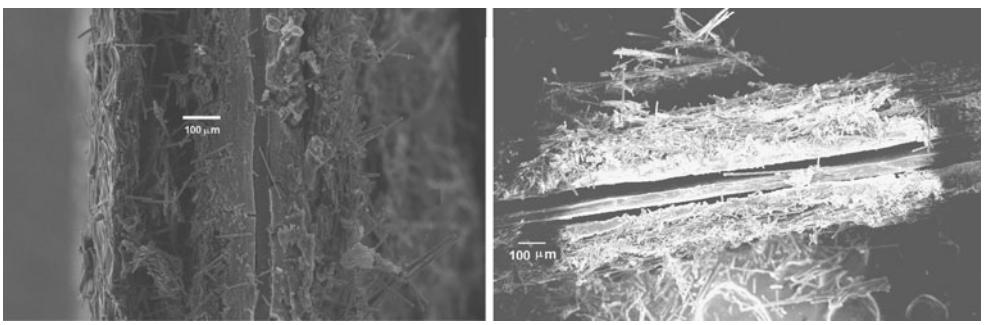

Fig. 7 SEM images of MEA with N112 (*left*) and with the SSC polymer (*right*) after long-term test

The decrease of conductivity due to membrane degradation in the low humidity condition has been explained by several authors. Chen and Fuller [16] have observed a strong decrease in Nafion® 112 thermal stability after a 120-h fuel cell OCV durability test at low humidity (RH 36%). In particular, pinholes and delamination were observed near the anode side and close to the centre. In addition, a significant decrease of membrane thickness from the nominal 50 to 35 μm was observed together with an 8.3% reduction in the ion exchange capacity that they attributed to side chain degradation due to the S–O–S cross-linking [16]. By using SEM analysis (Fig. 7), we have found a final average thickness of 35±3 μm for N112 with a 10% reduction with respect to that measured on the starting MEA after the hot pressing process (39 μm) or on a N112 dried at 110 °C for 1 h [17]. In the case of the SSC polymer, we have found a final average thickness of 24± 3 μm with a 30% reduction with respect to that measured on the MEA after the hot pressing process (34 μm).

It can then be concluded that the SSC polymer undergoes a higher mass loss than N112 with a 20% increase of rate degradation. Such thickness reduction higher than that attributed simply to drying should be ascribed to a real mass loss, as already proposed by the above-cited authors [16]. By means of ex situ hygrothermal ageing on Nafion® 112 for 400 days, Collette et al. [18] have reported membrane degradation through the modification of sulfonic acid end-groups consisting in the formation of sulfonic anhydride from condensation. Substitution of ionic-end group by less hydrophilic anhydrides leads to a significant decrease of water uptake and conductivity, as evidenced in our previous measurements.

Although the SSC polymer demonstrated to be more conductive, especially in the first hours as previously reported [9], it showed a weaker stability in long-term tests with a sharp performance decrease in low RH conditions. We cannot exclude the influence of the side chain chemical structure on the different degradation rates for the two polymers. In addition, it can be supposed that the higher SSC degradation rate was also related to its different mechanical properties, as reported by several authors [19–21]. In fact, during a normal fuel cell operation, the electrodes are pressed against the polymer electrolyte membrane, and that leads to a mechanical stress on the polymer. It is well known that the temperature and humidity influence strongly the mechanical properties of these materials (tensile modulus, stress, elongation at break, tear resistance, etc.) [20–23]. Ghielmi et al. [9] have reported that only the tear resistance seems to be the same for N112 and SSC. On the other hand, typical data of tensile modulus at low RH (50%) and 23 °C are 249 and 137 MPa for N112 and SSC polymer, respectively [19, 20]. In the same operative conditions, stress at break values in the machine and transverse directions (MD/TD) are 43/32 and 30/23 MPa for N112 and SSC polymer, respectively [19, 20]. Such data from the literature evidenced a different mechanical resistance, which is higher for N112 with respect to the SSC polymer in low RH conditions.

Fluoride emission and the water-related conductivity measured in the exhaust-collected water at the anode and cathode (Table 1) confirmed the previous results evidencing a strong correlation between the membrane mass loss in the exhaust-collected water and the degradation rate.

A second important change depicted in the Nyqvist plot (Figs. 3 and 4) was the increase of the first arc at high frequency (3–5 kHz) as a function of time. From the interpretation provided by the electric circuit model, this peak growth observed for both MEAs in the Bode plot (Fig. 8) is due to the fast charge transfer phenomena related to the electrodes kinetic (mainly the ORR). The product $R_{ct}C_{dl}$ (see circuit in Fig. 1) represents the time constant ($\tau = RC$), which is inversely related to the maximum frequency ($f_{max}=1/\tau$). This relation implies that the RC product remains constant during the long-term degradation test. This effect can be explained considering the presence of Nafion® in the catalytic layer composition. As reported previously [24], electrode impregnation with a proton conductor extends the three-dimensional reaction zone. An optimum Nafion® content in the electrode is necessary to minimize the charge transfer resistance, as well as the ionic and gas transport limitations. Nafion® long-term degradation due to low humidification occurred not only in the bulk membrane, but also in the catalytic layer, thus reducing its active content and decreasing the three-dimensional reaction zone [1, 25]. This reduction implies a symmetric increase of R_{ct} and a decrease of C_{dl} keeping their product constant. Obviously, the reaction zone reduction could also be ascribed to platinum dissolution and/or particle growth but, as has been demonstrated extensively by many authors [1, 2, 25], the dominant degradation mechanisms at low RH conditions are related to the membrane and ionomer. In addition, our

Table 1 Fluoride emission and water-related conductivity measured in exhaust-collected water

Type	$[F^-]$ (ppm) Cathode	$[\chi]$ ($\mu S cm^{-1}$) Cathode	$[F^-]$ (ppm) Anode	$[\chi]$ ($\mu S cm^{-1}$) Anode	Degradation rate ($\mu V h^{-1}$) (600 h)
Nafion™ 112	0.40	6.7	0.47	18.7	−154
SSC polymer	1.96	18.8	2.26	31.1	−471

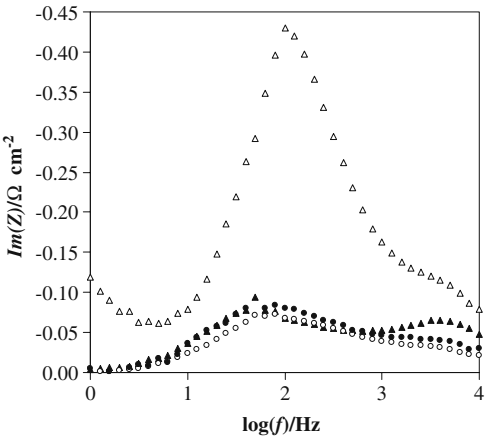

Fig. 8 Bode plot of MEA with N112 (*triangle*) and the SSC polymer (*circle*) at 50 °C and 250 mA/cm^2 after 40 h (*empty triangle* and *empty circle*) and 734 h (*filled triangle* and *filled circle*)

previous long-term testing [26, 27] of the same types of electrode at higher RH showed that the contribution of particle growth to degradation mechanism is very low. Adreaus and Scherer [28] have hypothesized that the loss of active surface at low RH occurred mainly on the anode. We can suppose that the lack of water at the anode increases the electro-osmotic drag, which leads to a dramatic increase of the membrane dehydration effect.

The second arc in the Nyquist plot evidenced by peaks at low frequency (50–100 Hz) is related to the mass transport phenomena (Fig. 8). $Z_w(0)$ obtained from fitting the experimental data for N112 showed to have a small reduction only in the activation phase (150–200 h) and then a constant value (235±7 mΩcm^2), thus evidencing no long-term effect due to low RH on the O_2 and H_2 diffusion phenomena into the electrodes.

On the other hand, the $Z_w(0)$ term for the SSC polymer was not constant and began to increase sharply after 273 h (1,100 mΩcm^2), thus indicating a strong diffusion problem. We can hypothesize that this problem is related to the transport of species in the catalytic layer due to a discontinuity between the SSC membrane and Nafion® ionomer (see Fig. 7). Nevertheless, the results led us to suppose that a sudden collapse of the electrode structure (diffusive and catalytic layers) onto the SSC membrane due to a fast thickness reduction has occurred. This structure collapse created a strong diffusive problem and $Z_w(0)$ increased.

The polarization curve (Fig. 9) confirmed these results showing a different decay profile for the two systems, starting from a similar performance at 156 h for N112 and 96 h for the SSC membrane. After a long-term test, both systems showed an increase of the slope in the linear region, characteristic of an increase of membrane resistance. In addition, the SSC membrane was characterized by a sharp fall due to the presence of limiting diffusion phenomena that probably caused the hypothesized structure to collapse in low RH conditions.

Conclusion

The results presented in this work evidenced a strong effect of low relative humidity on the lifetime of commercial polymer membranes. Long-term tests carried out at low humidification showed several effects, especially in the polymer. Prolonged dehydration produced a decrease of the three-dimensional reaction zone due to ionomer degradation in the catalytic layer and a continuous mass loss in the membrane evidenced by a thickness decrease and exhaust water contamination. This general effect was more prominent in the SSC membrane probably because of its different structure with a low equivalent weight, short side chain copolymer and weaker mechanical properties with respect to N112. Further studies are, however, needed to understand the relation between the decay rates and the polymer chemistry in order to obtain membranes with enhanced properties capable of competing in the fuel cell market.

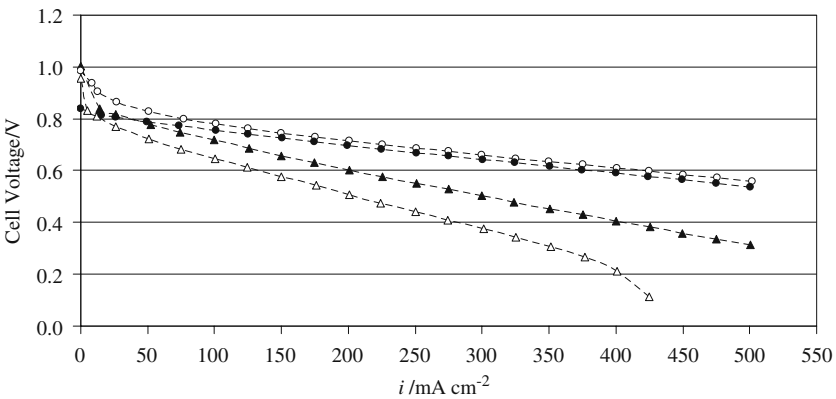

Fig. 9 Cell voltage vs. current density plot of MEA with N112 after 156 h (*filled circle*) and 1,019 h (*filled triangle*) and with the SSC polymer after 96 h (*empty circle*) and 734 h (*empty triangle*) at 50 °C

References

1. de Bruijn FA, Dam VAT, Janssen GJM (2008) Fuel Cells 08:3–22
2. Huang X, Solasi R, Zou Y, Feshler M, Reifsnider K, Condit D, Burlatsky S, Madden T (2006) J Polym Sci B Polym Phys 44:2346–2357
3. Schmittinger W, Vahidi A (2008) J Power Sources 180:1–14
4. Buchi F, Srinivasan S (1997) J Electrochem Soc 144(8):2767–2772
5. Yu J, Matsuura T, Yoshikawa Y, Islam MN, Hori M (2005) Electrochem Solid-State Lett 8(3):A156–A158
6. Nakayama H, Tsugane T, Kato M, Nakagawa Y, Hori M (2006) Fuel cell seminar abstracts. Courtesy Associates, Hawaii
7. Wahdame B, Candusso D, François X, Harel F, Péra MC, Hissel D, Kauffmann JM (2007) Int J Hydrogen Energy 32:4523–4536
8. Arcella V, Troglia C, Ghielmi A (2005) Ind Eng Chem Res 44:7646–7651
9. Ghielmi A, Vaccarono P, Troglia C, Arcella V (2005) J Power Sources 145:108–115
10. Merlo L, Ghielmi A, Cirillo L, Gebert M, Arcella V (2007) Sep Sci Technol 42:2891–2908
11. Silva RF, Passerini S, Pozio A (2005) Electrochim Acta 50:2639–2645
12. Mura F, Silva RF, Pozio A (2007) Electrochim Acta 52:5824–5828
13. Giorgi L, Antolini E, Pozio A, Passalacqua E (1998) Electrochim Acta 43:3675–3680
14. Yuan X, Wang H, Sun JC, Zhang J (2007) Int J Hydrogen Energy 32:4365–4380
15. Danzer MA, Hofer EP (2009) J Power Sources 190:25–33
16. Chen C, Fuller TF (2009) Polym Degrad Stab 94:1436–1447
17. Silva RF, De Francesco M, Pozio A (2004) J Power Sources 134:18–26
18. Collette FM, Lorentz C, Gebel G, Thominette F (2009) J Membr Sci 330:21–29
19. Grot W (2007) Fluorinated Ionomers. William Andrew Publishing, New York, p 53
20. Tang Y, Karlsson AM, Santare MH, Gilbert M, Cleghorn S, Johnson WB (2006) Mater Sci Eng A 425:297–304
21. Kundu S, Simon LC, Fowler M, Grot S (2005) Polymer 46:11707–11715
22. Satterfield MB, Majsztrik PW, Ota H, Benziger JB, Bocarsly AB (2006) J Polym Sci B 44:2327–2345
23. Bauer F, Denneler S, Willert-Porada M (2005) J Polym Sci B 43:786–795
24. Antolini E, Giorgi L, Pozio A, Passalacqua E (1999) J Power Sources 77:136–142
25. Xie J, Wood DL III, More KL, Atanassov P, Borup RL (2005) J Electrochem Soc 152:A1011–A1020
26. Pozio A, Silva RF, De Francesco M, Giorgi L (2003) Electrochim Acta 48:1543–1549
27. Silva RF, Pozio A (2007) J Fuel Cell Sci Technol 4:116–122
28. Andreaus B, Scherer GG (2004) Solid State Ionics 168:311–320